energy&fuels

ARTICLE

pubs.acs.org/EF

Effect of Additives on Decomposition of Sodium Carbonate: Precombustion CO_2 Capture Sorbent Regeneration

Ranjani V. Siriwardane,*[,†] James A. Poston, Jr.,[†] Clark Robinson,[†,‡] and Thomas Simonyi[†,‡]

[†]National Energy Technology Laboratory, United States Department of Energy, 3610 Collins Ferry Road, Post Office Box 880, Morgantown, West Virginia 26507-0880, United States

[‡]Parsons Infrastructure and Technology Group, Post Office Box 618, Pittsburgh, Pennsylvania 15129, United States

ABSTRACT: The effect of various additives on the decomposition of sodium carbonate (Na_2CO_3) was evaluated using temperature-programmed desorption, thermogravimetric analysis, X-ray diffraction, and X-ray photoelectron spectroscopy. Incorporation of additives, CaO and $Ca(OH)_2$, had a significant effect on lowering the decomposition temperature of Na_2CO_3, while $CaCO_3$, SiO_2, and Al_2O_3 had no effect. The amount of additive, sweep gas flow rate, and heating rate were also found to play a significant role in altering the decomposition temperature of Na_2CO_3. The formation of a carbonate-type intermediate in the presence of CaO and $Ca(OH)_2$ may have promoted the decomposition of Na_2CO_3.

INTRODUCTION

The world's energy supply is presently dominated by fossil fuels, with coal, petroleum, and natural gas supplying roughly 80% of the global primary energy demand.[1] One of the many environmental detriments resulting from the extraction, production, and use of fossils fuels that has recently come to the forefront is the generation of greenhouse gases, with the combustion of fossil fuels being a major source of carbon dioxide (CO_2).[2] Until the advent of advanced sustainable energy sources, technologies are needed that will allow use of fossil fuels while reducing greenhouse gas emissions. Existing commercial CO_2 capture technology is very expensive and energy-intensive. Improved technologies for CO_2 capture are necessary to achieve low energy penalties and reduce costs. Pressure swing adsorption (PSA)/sorption (PSS) and temperature swing adsorption (TSA)/sorption (TSS) are some of the potential techniques that could be applicable for removal of CO_2 from gas streams.[3,4]

According to a system analysis conducted in the Netherlands,[5] the PSA/TSA systems would be even more energy-efficient for integrated gasification combined cycle (IGCC) systems if the sorbents were operational at warm gas temperatures (250−350 °C; 0 °C = 273.15 K). Various alkali oxides and salts are potential candidates for the CO_2 capture process at these temperatures.[6−8] National Energy Technology Laboratory (NETL) researchers have developed NaOH- and $Mg(OH)_2$-based sorbents to remove CO_2 at warm gas temperatures.[9,10] Removal of CO_2 with alkali oxides and salts involves a chemical reaction that results in the formation of alkali carbonates. Regeneration of these materials requires high temperatures because it involves the decomposition of the alkali carbonates formed during absorption. The high regeneration energies of these sorbents would result in significant loss in system efficiency. Therefore, it is necessary to find a low energy regeneration procedure to be able to use CO_2 removal sorbents effectively. Incorporation of various additives may result in the decomposition of alkali carbonate at lower temperatures. This research focused on understanding the effect of additives on the decomposition of sodium carbonate; the results of which are described in this paper.

Several studies on the additive effect on carbonate decomposition have been reported. Doping effects of altervalent cations on the thermal decomposition and electrical conduction properties of manganese(II) carbonate ($MnCO_3$) have been studied by Hassan et al.[8] They observed that doping $MnCO_3^{II}$ carbonate with Li^+ and Al^{3+} ions enhanced the decomposition of the carbonate. The authors explained that this enhanced effect is due to the generation of hole defects, which are concentrated at the reaction interface. The doping effect of Li^+ is more pronounced than that of the Al^{3+} ions.

Wigmans et al.[11] conducted a temperature-programmed desorption (TPD) study on carbonate decomposition in the presence of carbon. They observed enhancement of sodium carbonate (Na_2CO_3) decomposition by carbon. They indicated that the mechanism includes decomposition to Na_2O and subsequent reduction to Na metal. Addoun et al.[12] studied the effect of alkali carbonate decomposition on the porosity of carbons. They observed that the nature of the cation affected the degree of microporosity in the following order: Li < Na < K < Rb < Cs. The highest effects observed with Cs, Rb, and K are due to the decomposition of Cs, Rb, and K carbonates on the carbon surface at a rather low temperature ($T \sim 227$ °C or 500 K) because of the formation of alkaline oxide clusters and a high degree of dispersion of the alkaline compound.

Kim et al. studied the effect of SiO_2 on the decomposition of Na_2CO_3.[13] They observed that the addition of SiO_2 greatly enhanced the decomposition of Na_2CO_3. The initial decomposition product was identified as Na_2SiO_3, irrespective of the mixing ratio of Na_2CO_3/SiO_2. Said et al. studied the influence of iron additions on the thermal decomposition of zinc carbonate.[14]

Received: November 3, 2010
Revised: January 18, 2011
Published: February 18, 2011

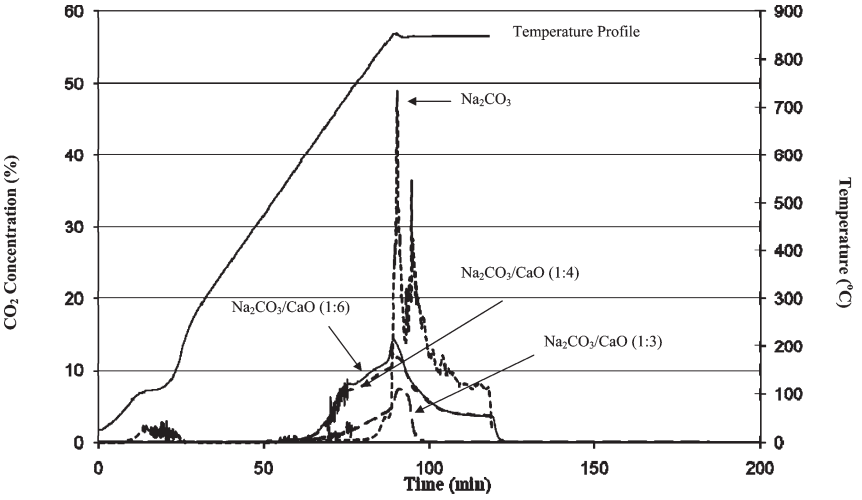

Figure 1. Effect of Na_2CO_3/CaO system composition on the thermal decomposition of Na_2CO_3.

They observed that the presence of iron retarded the decomposition. The retardation effect increased with an increasing ion concentration up to 50 atomic percent. The authors indicated that the presence of foreign ions causes lattice deformation, as well as either a change in the valence of ions or the appearance of additional cationic or anionic vacancies in the lattice, which, in turn, strongly affects the thermal decomposition rate. The authors also indicated that the introduction of iron ions into ZnO lattice positions during thermoanalysis decreased the hole concentration either on the surface or in the bulk. However, studies on the effect of sodium carbonate decomposition with additives used in present work are not reported in the literature.

EXPERIMENTAL SECTION

TPD studies were conducted in a lab-scale fixed-bed flow reactor (Micromeritics Autochem 2910 atmospheric flow reactor) at 14.7 psi ($\sim 1.01 \times 10^5$ Pa). The outlet gas stream was analyzed using a Pfeiffer Vacuum Thermostar mass spectrometer. In the TPD studies, N_2 was introduced to the samples (1.7×10^{-3} L) at a flow rate of 10 cm^3/min and the temperature was increased at a rate of 10 °C/min while measuring the CO_2 concentration with the mass spectrometer. For comparison, in some TPD studies, a nitrogen flow rate of 50 cm^3/min and heating rates of 5 and 25 °C/min were used.

Thermogravimetric analysis (TGA) experiments were conducted on a TA Instruments model 2050 thermogravimetric analyzer. Samples (90 mg) were heated to 850 °C under N_2, and weight gain was recorded isothermally as a function of time. N_2 was introduced at a flow rate of 90 cm^3/min, and the temperature was increased at a rate of 10 °C/min up to 850 °C and held isothermally for 120 min.

High-temperature *in situ* X-ray diffraction (XRD) studies were carried out using an Anton Paar HTK 1200N high-temperature stage connected to an Anton Paar TCU-1000N temperature control unit. The high-temperature stage was interfaced to a Panalytical PW 3040 X-Pert Pro XRD system equipped with a 50 kV PW 3373/00 Cu LFF high-power ceramic tube with a Cu anode and a PW 3011/20 detector. The X-ray wavelength used was Cu $K\alpha_1$ at 1.540 56 Å. System calibration was carried out using a polysilicon-pressed disk with Si ⟨111⟩ referenced to 28.443° (2θ). Sample data were acquired at 45 kV and 40 mA in a line focus mode. The *in situ* high-temperature studies were conducted in ambient air, with data analysis carried out using X'Pert Highscore Plus software supplied by Panalytical. For comparative purposes, in addition to the Na_2CO_3−CaO sample, *in situ* temperature studies were also carried out with a CaO sample from ambient temperature (21 °C) to 400 °C and with a Na_2CO_3 sample from ambient temperature (21 °C) to 650 °C.

X-ray photoelectron spectroscopy (XPS) was carried out using a Physical Electronics (PHI) model 3057 X-ray photoelectron spectroscopy subsystem with a spherical capacitance analyzer and a model 04-548 X-ray source. The system consists of separately pumped preparation and detection chambers that are routinely operated within the pressure range of 10^{-8}−10^{-10} Torr (from 1.3×10^{-6} to 1.3×10^{-8} Pa). The system was calibrated in accordance with PHI procedures,[15] with photoemission lines E_b of Cu $2p_{3/2}$ = 932.7 eV and E_b of Au $4f_{7/2}$ = 84 eV, using an aluminum anode. All reported intensities are experimentally determined peak areas divided by the instrumental sensitivity factors. The binding energies were corrected for sample charging using the reference binding energy (BE) of adventitious C (1s) as 284.6 eV.[15]

The spectrometer sample holder is resistively heated and capable of withstanding temperatures up to 600 °C. The sample preparation chamber is separated from the main analysis chamber by a gate valve. The samples were placed in the preparation chamber, evacuated, and then heated. After the preparation chamber reached the desired pressure, the sample was transferred to the analyzing chamber for data acquisition. The sample was maintained at the desired temperature throughout the experiment, including data acquisition. The data were analyzed with analysis software developed by RBD Instruments.

The chemicals used in these series of experiments were obtained from Alfa Asear (Johnson Matthey). The sodium carbonate used in the TPD, TGA, and XRD studies was monohydrated ($Na_2CO_3 \cdot H_2O$). The calcium oxide and calcium carbonate used were anhydrous. The sodium carbonate used in the XPS studies was also anhydrous.

RESULTS

TPD. The measured CO_2 concentration and corresponding temperature data as a function of time during TPD measurements of $Na_2CO_3 \cdot H_2O$/CaO mixtures with varying compositions are shown in Figure 1. For pure $Na_2CO_3 \cdot H_2O$, the increase in the CO_2 concentration initiates around 780 °C and the CO_2 maximum occurs around 850 °C, with a narrow CO_2 peak. When $Na_2CO_3 \cdot H_2O$ was mixed with CaO in the ratio of 1:3 $Na_2CO_3 \cdot H_2O$/CaO, the increase in the CO_2 concentration initiated at around 550 °C, a temperature that is significantly lower than that of pure $Na_2CO_3 \cdot H_2O$. The CO_2 curve was also broader than that of pure $Na_2CO_3 \cdot H_2O$, indicating not only that CO_2

dx.doi.org/10.1021/ef101486m |*Energy Fuels* 2011, 25, 1284–1293

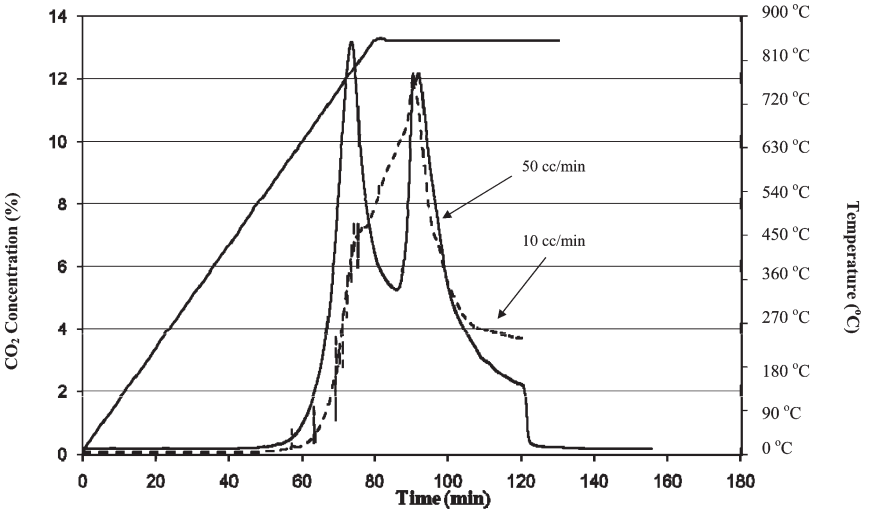

Figure 2. Effect of the flow rate on $Na_2CO_3 \cdot H_2O$/CaO (1:4) thermal decomposition.

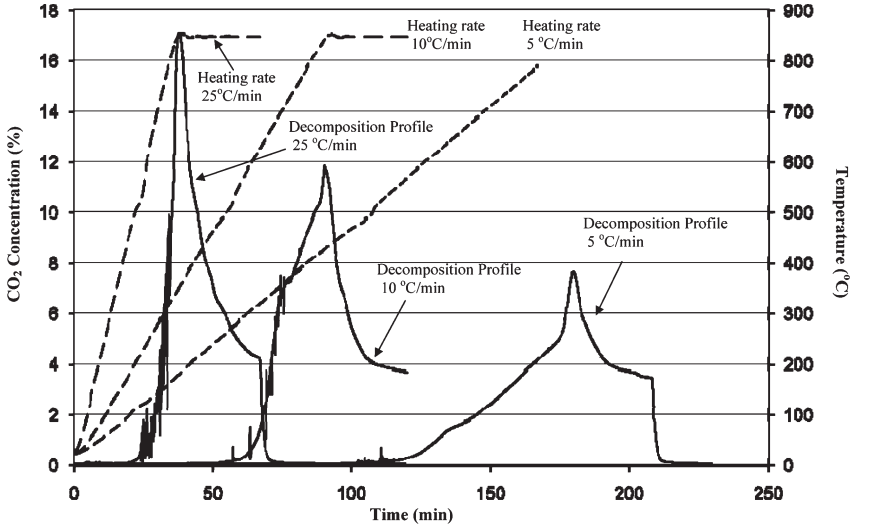

Figure 3. Effect of the heating rate on $Na_2CO_3 \cdot H_2O$/CaO (1:4) thermal decomposition.

decomposition initiates around 550 °C but also that it continues at a wide range of temperatures. When the $Na_2CO_3 \cdot H_2O$ concentration was further decreased to 1:4 $Na_2CO_3 \cdot H_2O$, CO_2 was initially observed around 520 °C because of the decomposition of carbonate, with more CO_2 being observed in the 520 °C temperature range than that observed with the $Na_2CO_3 \cdot H_2O$/CaO (1:3) sample. The CO_2 curve for the $Na_2CO_3 \cdot H_2O$/CaO (1:6) sample was similar to that of the 1:4 samples. For these three Na_2CO_3/CaO systems, an increase in the CaO concentration in the $Na_2CO_3 \cdot H_2O$/CaO mixture results in a decrease in the decomposition temperature of Na_2CO_3, with an optimum CaO concentration beyond which the decomposition temperature of Na_2CO_3 is not affected.

The effect of the N_2 flow rate on the decomposition of $Na_2CO_3 \cdot H_2O$/CaO (1:4) is shown in Figure 2. At 10 cm^3/min flow rate, the CO_2 decomposition initiates around 550 °C, with a secondary peak observed at 718 °C and a maximum peak observed around 850 °C. At a flow rate of 50 cm^3/min N_2, two distinct desorption peaks were observed. The decomposition temperature and intensity of the peak observed initially at 850 °C remained essentially unchanged. The CO_2 concentration of the secondary peak was found to increase. A small temperature difference between the low-temperature peaks was also observed. This observation suggests that higher flow rates may facilitate a lower carbonate decomposition temperature through the increased removal of CO_2 from the gas stream. The two peaks observed at each flow rate represent two types of absorption sites from which CO_2 production is thermodynamically favorable. As observed from Figure 2, the flow rate has little effect on the desorption peak at 850 °C but does have a significant effect on the lower temperature desorption peak.

The effect of the heating rate on the decomposition of $Na_2CO_3 \cdot H_2O$/CaO (1:4) is shown in Figure 3. The initial decomposition temperature appears to be similar for all heating rates; however, the shape of the CO_2 concentration curve was affected by the heating rate. A sharp curve was observed at a heating rate of 25 °C/min, with a peak maximum at 850 °C. When the heating rate was decreased to 10 °C/min, a secondary peak appeared around 725 °C. When the heating rate was further decreased to 5 °C/min, the secondary peak appeared at a

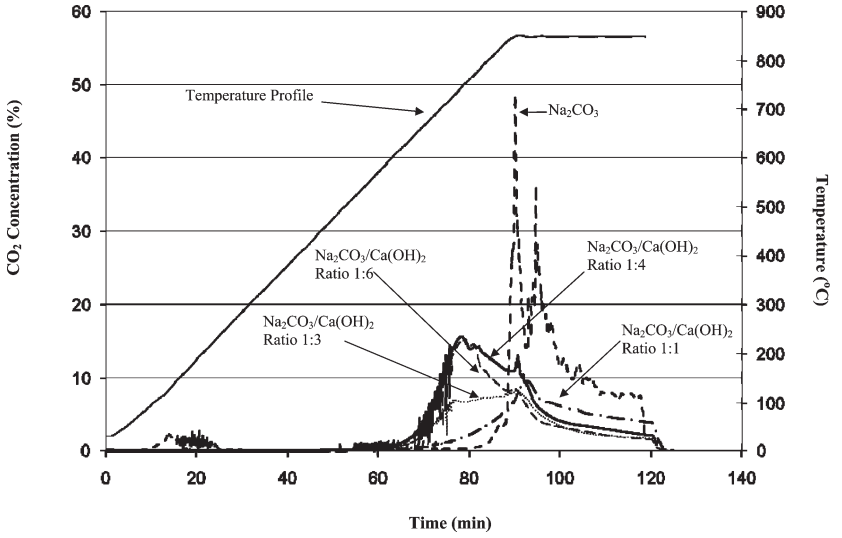

Figure 4. Effect of $Na_2CO_3 \cdot H_2O/Ca(OH)_2$ composition on Na_2CO_3 thermal decomposition.

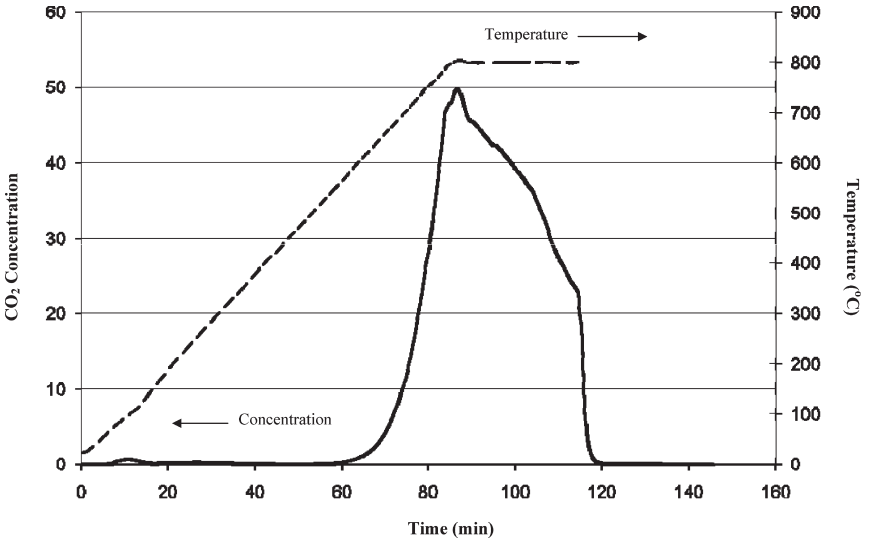

Figure 5. Effect of $CaCO_3$ addition on Na_2CO_3 thermal decomposition.

temperature of 625 °C. Subsequently, a lower heating rate appears to facilitate Na_2CO_3 decomposition at a lower temperature.

Because the addition of CaO decreased the decomposition temperature of Na_2CO_3, the effect of the addition of $Ca(OH)_2$ was also investigated. The CO_2 decomposition curves for various $Na_2CO_3 \cdot H_2O/Ca(OH)_2$ compositions are shown in Figure 4. After the addition of $Ca(OH)_2$, the initial decomposition temperature of Na_2CO_3 decreased from 785 to 550 °C, similar to the observations with CaO. However, the shapes of the CO_2 curves with $Ca(OH)_2$ during decomposition of the carbonate were significantly different from those of Na_2CO_3 and Na_2CO_3/CaO. Unlike the TPD curve for pure $Na_2CO_3 \cdot H_2O$, which had a sharp maximum at 850 °C, the $Na_2CO_3 \cdot H_2O/Ca(OH)_2$ (ratio 1:1) CO_2 peak maximum still appeared at 850 °C, but the peak was broad. With a $Na_2CO_3 \cdot H_2O/Ca(OH)_2$ ratio of 1:3, a very broad maximum between 725 and 850 °C was observed. When the $Na_2CO_3 \cdot H_2O/Ca(OH)_2$ ratio was increased to 1:4, the maximum appeared at 750 °C, with the peak being narrower than that for the 1:3 ratio. Thus, the addition of $Ca(OH)_2$ appears to be more effective than the addition of CaO in lowering the decomposition temperature of Na_2CO_3.

When $CaCO_3$ was added to $Na_2CO_3 \cdot H_2O$ (Figure 5), the temperature of decomposition did not initiate at 550 °C, as was observed with CaO and $Ca(OH)_2$. Similarly, when $Na_2CO_3 \cdot H_2O$ was mixed with Al_2O_3 and SiO_2, lower decomposition temperatures were not observed, as shown in Figure 6. Thus, CaO and $Ca(OH)_2$ have a unique ability to affect the decomposition temperature of Na_2CO_3.

TGA. Thermogravimetric data for the decomposition of pure $Na_2CO_3 \cdot 1H_2O$, pure CaO, and a mixture of $Na_2CO_3 \cdot H_2O$/CaO (1:3) are summarized in Table 1. When pure CaO was heated to 800 °C, about 4.6 wt % was lost between 288 and 405 °C and 1.2 wt % was lost between 405 and 657 °C, believed to be due to the loss of H_2O. When pure $Na_2CO_3 \cdot H_2O$ was heated to 800 °C, about 14.8 wt % was lost between 62 and 163 °C, which is close to the calculated amount of water from the formula (14.5 wt %). No significant weight was lost after 162 °C. This observation indicates that carbonate decomposition takes place above 800 °C.

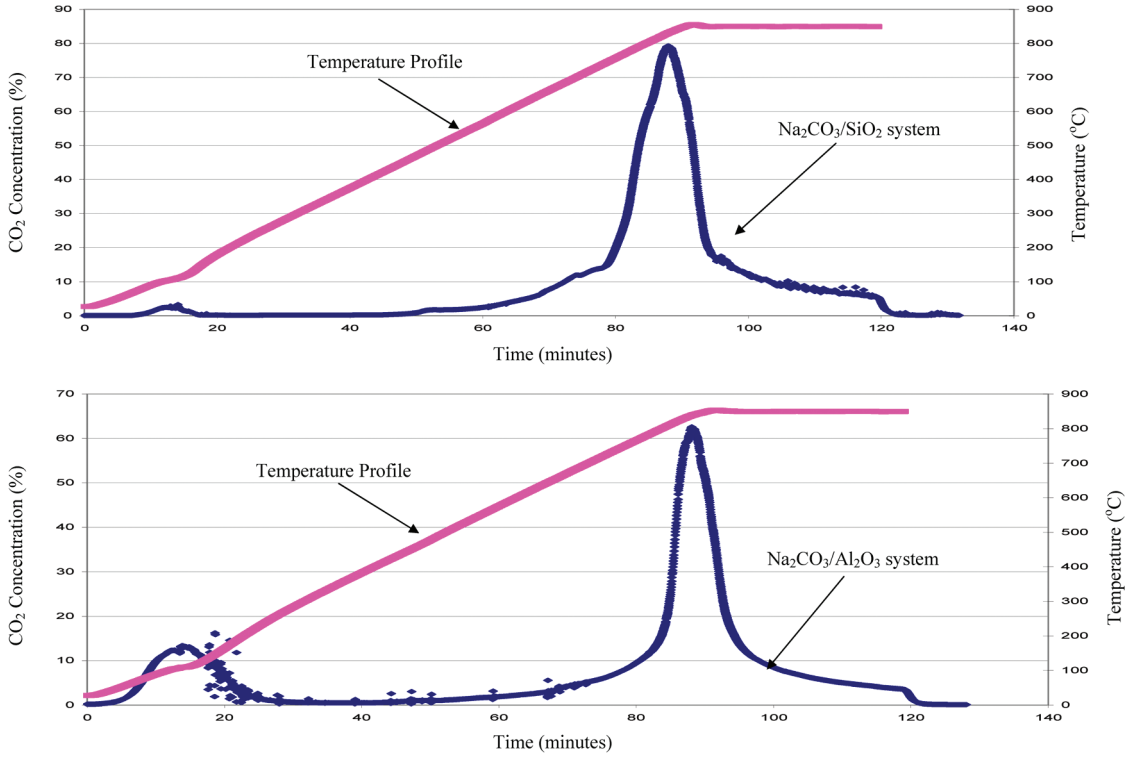

Figure 6. Effect of (a) SiO_2 and (b) Al_2O_3 addition on Na_2CO_3 decomposition.

Table 1. Weight Loss as a Function of the Temperature (°C) of CaO, $Na_2(CO_3)\cdot H_2O$, and Selected $Na_2(CO_3)\cdot H_2O$/CaO Systems

compound	temperature (°C)	Δwt (%)	temperature (°C)	Δwt (%)	temperature (°C)	Δwt (%)	temperature (°C)	Δwt (%)
CaO	288−405	4.6	405−657	1.2	>657	0		
$Na_2CO_3\cdot H_2O$	062−163	14.8	162−800	0.3				
$Na_2CO_3\cdot H_2O$/CaO ratio 1:3	033−337	2.5	337−439	15.3	439−652	5.1	652−800	2.6
$Na_2CO_3\cdot H_2O$/CaO ratio 1:3	045−344	2.6	344−436	15.1	436−700	4.5	700	1.5

For the $Na_2CO_3\cdot H_2O$/CaO (1:3) system, the initial weight loss was 2.5% at temperatures between 33 and 337 °C. A repeated test produced results of 2.6% initial weight loss at temperatures between 45 and 344 °C. This weight loss is believed to be due to the loss of water (H_2O). The percent of H_2O calculated from the formula is about 6 wt %, indicating that all H_2O was not removed fully at 337/344 °C. For the $Na_2CO_3\cdot H_2O$/CaO (1:3) system, the major weight loss was observed to be between the temperatures 337 and 439 °C during repeated tests, with an approximate weight loss of 15%, indicating that additional H_2O loss and carbonate decomposition may have taken place in this temperature range. It appears that carbonate decomposition initiates around 337−439 °C with the $Na_2CO_3\cdot H_2O$/CaO (1:3) system. It is difficult to determine the exact starting temperature of carbonate decomposition, because some H_2O loss may have occurred in that temperature range. The weight loss as a result of carbonate decomposition continued from 439 to 652 °C and from 436 to 700 °C, respectively, followed by slow decomposition after 652 °C up to 800 °C for the test. During the repeated test, the time at 800 °C was extended, which resulted in additional weight loss. The total weight loss was 25.5% up to 800 °C and 23.7% up to 700 °C during repeated tests. The theoretical weight loss combined with both H_2O loss and carbonate decomposition calculated from the formula was about 26.7%, a value close to that of the experimentally determined value. This indicates that, for $Na_2CO_3\cdot H_2O$/CaO, the carbonate decomposition takes place below 800 °C, which is different from that of pure $Na_2CO_3\cdot H_2O$. These data are consistent with the TPD and XRD data that will be discussed later.

XRD. Analysis of the CaO *in situ* high-temperature XRD data showed that the sample is composed of the CaO phase from 21 to 400 °C, with the presence of $Ca(OH)_2$ appearing at 150 °C and disappearing at 400 °C. Analysis of the Na_2CO_3 standard at 21 °C revealed the sample to be $Na_2CO_3\cdot H_2O$. The peak shape, full width at half-maximum (fwhm), and poor reference fit indicated that the material was not entirely crystalline. The presence of Na_2CO_3 was observed upon heating the sample to 100 °C and continued to be observed through 300 °C. From 350 to 650 °C, it was difficult to observe the presence of Na_2CO_3 because of the poor reference match for the main diffraction patterns. The peak shape, fwhm, and poor reference fit indicated

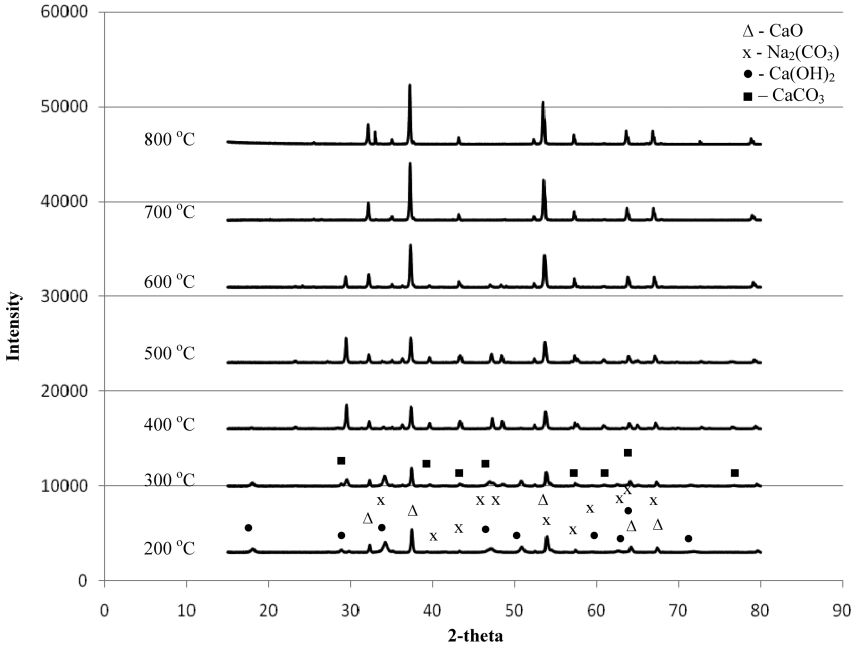

Figure 7. *In situ* high-temperature XRD data from the $Na_2CO_3 \cdot H_2O/CaO$ (1:3) system.

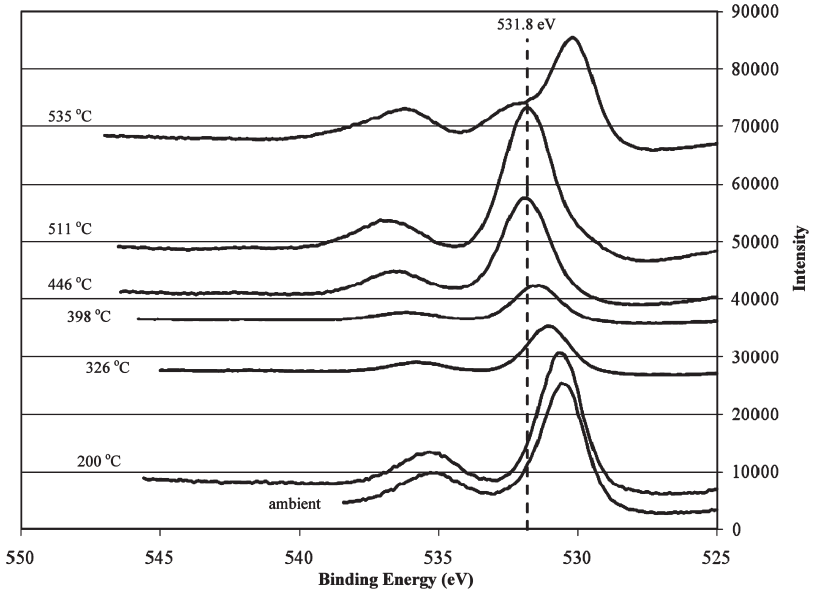

Figure 8. O 1s region of Na_2CO_3 during heating.

that the sample was disordered and not entirely crystalline. The presence of an oxide was not observed.

XRD *in situ* temperature studies on the $Na_2CO_3 \cdot H_2O/CaO$ (1:3 ratio) sample were carried out from ambient temperature (21 °C) to 800 °C (Figure 7). Analysis of the $Na_2CO_3 \cdot H_2O/CaO$ (1:3) sample at ambient temperature showed the sample to be composed primarily of CaO and $Ca(OH)_2$ with a small concentration of $Na_2CO_3 \cdot H_2O$. The definitive presence of Na_2CO_3 was not observed at any temperature ranging from 100 to 800 °C, indicating that the $Na_2(CO_3)$ material was disordered and not entirely crystalline. No presence of any other Na-based compound could be identified from 300 to 800 °C.

The formation and presence of $CaCO_3$ was observed from 300 to 600 °C. At 700 and 800 °C, the only Ca-based compound observed was CaO, although the reference fit was poor, indicating that the sample was disordered. At no temperature (21−800 °C) was the formation of any crystalline Na−Ca-type compound observed.

XPS Analysis. *In situ* high-temperature XPS analysis was conducted on Na_2CO_3 and a mixture (1:3) of Na_2CO_3/CaO. The sample was heated in the sample preparation chamber to the desired temperature, with a standing pressure of 10^{-6}−10^{-7} Torr, and was transferred to the analysis chamber for data acquisition while maintaining temperature.

The O 1s spectral region for Na_2CO_3 (Figure 8) contained one distinct peak centered at 530.5 eV. The BE value of the O 1s peak centered at 530.5 eV is considerably lower than that reported in the literature for Na_2CO_3,[16−18] suggesting that the

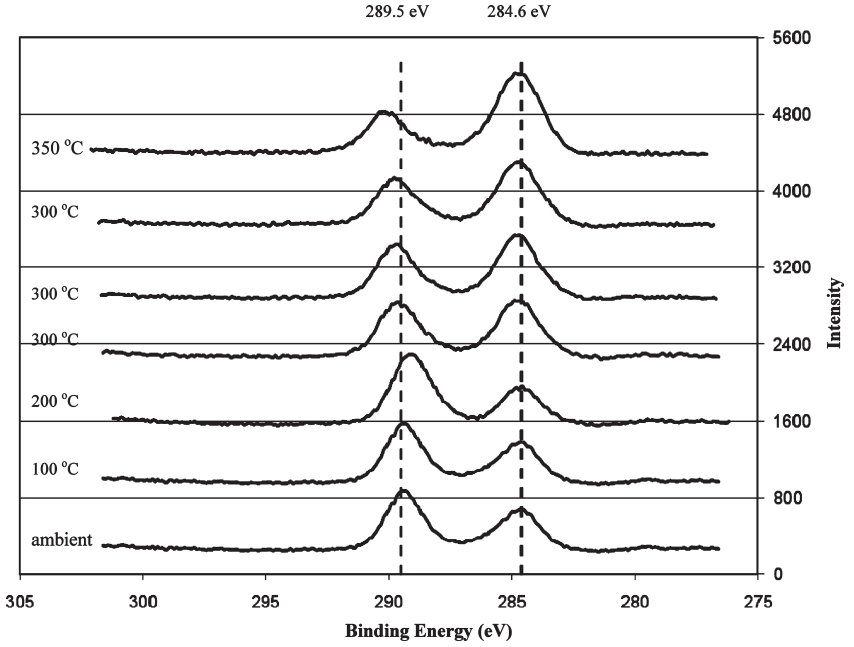

Figure 9. C 1s region of the Na_2CO_3/CaO (1:3) system during heating.

surface composition of the $Na_2(CO_3)$ standard may have been non-stoichiometric or in a hydroxide (OH^-) form. The O 1s BE value increased with an increased temperature approaching a value of 531.8 ± 0.1 eV, which corresponds to the oxygen in $Na_2(CO_3)$, between the temperature range of 398 and 511 °C.[16−18] At 533 °C, a decrease in the O 1s BE value to 530.3 eV was observed. The value of 530.3 eV is slightly higher than that reported in the literature (529.7 eV) for Na_2O.[18,19] The presence of a small peak corresponding to oxygen of carbonate indicated that complete decomposition had not taken place. This was also confirmed by the continued presence of the C 1s carbonate peak (not shown).

The C 1s spectral region of $Na_2(CO_3)$ at ambient temperature, consisted of two distinct peaks (not shown) centered at 289 and 284.6 eV. The C 1s BE value of 289 eV is lower than that reported in the literature for $Na_2(CO_3)$.[16,17] A similar temperature correlation was observed in the C 1s region as that observed in the O 1s region, with the C 1s carbonate peak approaching BE values consistent with those reported in the literature for carbonate at 326 °C during $Na_2(CO_3)$ decomposition.[16,17] At temperatures below 326 °C, the carbonate peak was the dominant peak with a ubiquitous carbon/carbonate carbon ratio (C_u/C_c) of approximately 0.5 and 0.4 for $Na_2(CO_3)$ at ambient and 204 °C, respectively. At 326 °C, the C_u/C_c ratio was approximately 0.8, indicating that the peak intensities were approaching equality. At 398 °C, the C_u/C_c ratio was approximately 1.4, indicating that the carbonate peak was no longer the dominant C 1s peak and that decomposition was underway. An increase in the carbonate BE value to 289.9 eV, a value slightly higher than that reported for $Na_2(CO_3)$, was observed.[16,17] The carbonate peak intensity continued to decrease with increased temperature, with corresponding BE values of approximately 290.1 ± 0.1 eV in the temperature range of 446−511 °C. At 511 °C, the presence of the C 1s ubiquitous peak was not observed. At 535 °C, the maximum temperature, the C 1s carbonate BE value increased to 290.6 eV, with the peak intensity being very low.

The BE value for the corresponding Na 1s peak (figure not shown) at ambient temperature was 1070 eV, a value less than that reported in the literature for $Na_2(CO_3)$.[16,17] This BE value is consistent with observations of the C 1s and O 1s spectral regions and further indicates that the surface composition is non-stoichiometric. The BE value of the Na 1s peak continued to increase with an increasing temperature up to 398 °C, where the Na 1s BE value approached that reported in the literature for $Na_2(CO_3)$.[16,17,20] This temperature is higher than the temperature observed in the C 1s and O 1s spectral regions (326 °C), where the corresponding BE values were in the range reported in the literature for $Na_2(CO_3)$.[16−18] This temperature difference is not fully understood but may be related to surface rearrangement. At 446 °C, the Na 1s BE value increased to 1071.9 eV, with the BE value remaining at 1071.9 ± 0.1 eV throughout the temperature at 535 °C, the maximum temperature.

Analysis of the Na_2CO_3/CaO mixture (1:3) at ambient temperature revealed two distinct peaks in the C 1s region (Figure 9) centered at BE values of 284.6 and 289.5 eV; values correlating to ubiquitous carbon and carbonate carbon.[15−17] The carbonate carbon peak was the dominant spectral peak. When the $Na_2(CO_3)$/CaO mixture was heated, no significant changes were observed until 200 °C, where a slight decrease in the carbonate C 1s spectral peak BE value to 289.2 eV was observed. The carbonate carbon peak in the C 1s region remained the dominant spectral peak. At 300 °C, the initial intensities of the ubiquitous carbon and carbonate carbon peaks were approximately equal, but with increased time, the intensity of the carbonate peak continued to decrease, making the ubiquitous carbon peak the dominant peak in the C 1s region, as shown in Figure 9. At 350 °C, the maximum temperature, the C 1s carbonate peak further decreased in intensity, indicating further decomposition, as well as a shift in BE to approximately 290.2 eV, indicating a non-stoichiometric surface.

In the O 1s region at ambient temperature, a single slightly broad and asymmetrical peak with a BE value of 531 eV was observed, as shown in Figure 10. Spectral deconvolution

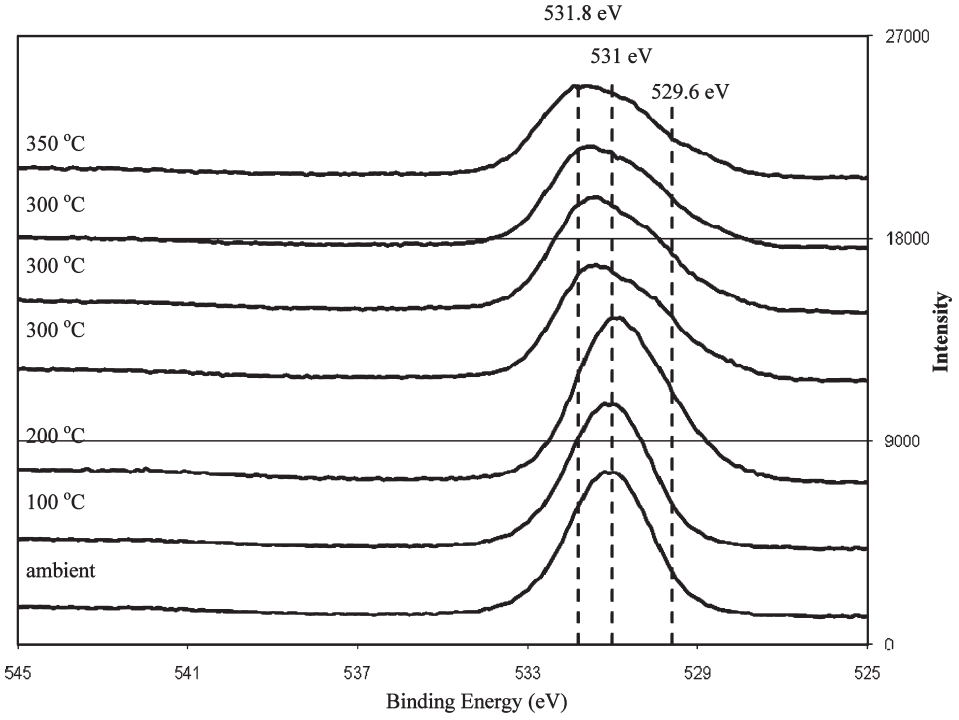

Figure 10. O 1s region of the Na_2CO_3/CaO (1:3) system during heating.

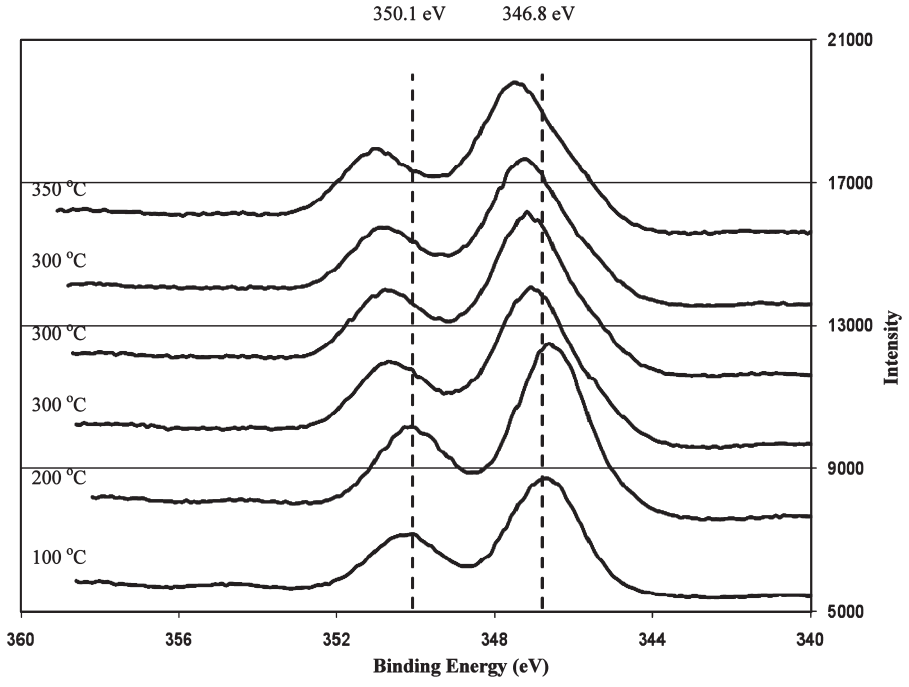

Figure 11. Ca 2p region of the Na_2CO_3/CaO (1:3) system during heating.

indicates that a secondary peak may be present at approximately 531.8 eV. A BE value of 531 eV is close to the value reported in the literature for CaO, and a BE value of 531.8 eV is close to the value of either $CaCO_3$ or $Na_2(CO_3)$.[16−18] The asymmetry and broadening of the O 1s peak, as shown in Figure 10, continued with both increasing time and temperature. At 300 °C, deconvolution indicates the formation of an additional peak at 529.6 eV, a value that correlates to values reported in the literature for Na_2O.[18,19] Increased time resulted in the increased formation of Na_2O. The broadness and asymmetry of the O 1s peak continued to increase at 350 °C.

Observation of the Ca 2p spectral region revealed two distinct peaks (Figure 11) in the Ca 2p region with BE values of 346.8 and 350.1 eV (Δ 3.4 eV), values close to that reported for CaO.[15,16,20−22] When the $Na_2(CO_3)$/CaO mixture was heated, changes observed in the Ca 2p region with temperature were different from those observed in the C 1s and O 1s regions, with significant changes not being observed until 300 °C, as shown in

dx.doi.org/10.1021/ef101486m |*Energy Fuels* 2011, 25, 1284–1293

Figure 11. At 300 °C, both a peak shift toward higher BE and an asymmetry on the lower BE side of the Ca $2p_{3/2}$ peak were observed. This shift toward higher BE continued with time, with a final BE value of 347.3 eV, a BE value that is slightly higher than that reported in the literature for $Ca(CO_3)$.[15,23,24] At 350 °C, the BE value of the Ca 2p peak further increased to 347.4 eV, a BE value higher than that reported for $Ca(CO_3)$.

The Na 1s spectral peak (not shown) was of low intensity and broad, with a BE value of 1071.3 eV, which correlates to $Na_2(CO_3)$.[16,17,20] Aside from a slight increase in intensity at 200 °C, the peak intensity decreased with both time and temperature. At 350 °C, the Na 1s peak was no longer observed. Given the low intensity of the Na 1s peak and the high intensity, asymmetry, and broadness of the O 1s peak, the dominant oxygen-containing species on the sample surface were not Na-based.

On the basis of the XPS spectroscopic data of the C 1s and O 1s region, the decomposition of pure $Na_2(CO_3)$ initiated around 398 °C, while for the $Na_2(CO_3)$/CaO mixture (1:3), the decomposition initiated at 300 °C. This observation indicates that the presence of CaO lowers the decomposition temperature of $Na_2(CO_3)$, which is consistent with the TGA and TPD data. These decomposition temperatures are significantly lower than those observed during decomposition at atmospheric pressure, because XPS analysis was conducted in vacuum as opposed to atmospheric pressure. Similar observations regarding lower decomposition temperatures in vacuum have been previously observed.[25,26]

DISCUSSION

The presence of both CaO and $Ca(OH)_2$ decreased the decomposition temperature of $Na_2(CO_3)$. XRD studies did not indicate the presence of any crystalline compounds formed between Na and Ca. However, the formation of $CaCO_3$-type species was observed from both XPS and XRD at intermediate temperatures prior to carbonate decomposition. Thus, the decomposition of $Na_2(CO_3)$ may be enhanced by CaO through the formation of an intermediate carbonate complex, as shown in reactions 1 and 2.

$$Na_2(CO_3) + CaO \leftrightarrow Na_2\cdots CO_3 - Ca\cdots O \quad (1)$$

$$Na_2\cdots CO_3 - Ca\cdots O \leftrightarrow Na_2O + CaO + CO_2 \quad (2)$$

$Ca(OH)_2$ had an even more pronounced effect on the decomposition temperature of $Na_2(CO_3)$ than that of CaO. The formation of NaOH may have facilitated the carbonate decomposition, as shown in reactions 3 and 4.

$$Na_2(CO_3) + Ca(OH)_2 \rightarrow 2NaOH\cdots CO_3\cdots Ca \quad (3)$$

$$2NaOH\cdots CO_3\cdots Ca \rightarrow H_2O + CaO + CO_2 \quad (4)$$

When $Ca(CO_3)$ was added to $Na_2(CO_3)$, the decomposition temperature did not change. The presence of carbonate in $Ca(CO_3)$ possibly hindered the formation of a Na···carbonate···Ca intermediate. This would indicate that the Ca···carbonate intermediate is important in facilitating the decomposition of $Na_2(CO_3)$.

It was also observed that the heating (temperature) rate and sweep gas flow rate had an effect on the thermal decomposition temperature of $Na_2(CO_3)$/CaO. A lower heating rate of 5 °C/min facilitated the faster decomposition of $Na_2(CO_3)$ initiating at a lower temperature, as opposed to heating rates of 10 and 25 °C/min. The lower heating rate results in increased resonance time at a given temperature range, which facilitates the $Na_2(CO_3)$ thermal decomposition process by driving reactions 1 and 2 and 3 and 4 farther to the right than would have been achieved under a higher heating rate. A higher sweep gas flow rate was also found to facilitate thermal decomposition of $Na_2(CO_3$/CaO). The peaks around 700 and 850 °C were observed at both flow rates; however, the peaks were more distinct, and the intensity of the 700 °C peak was greater at the higher flow rate. The two peaks observed at each flow rate represent two types of absorption sites where CO_2 desorption is favorable. We speculate that the low-temperature peak (~700 °C) represents $NaCO_3$···CaO decomposition, while that of the high-temperature peak (850 °C) represents $NaCO_3$ decomposition. Faster CO_2 removal from the product stream at a higher flow rate may have facilitated the Na_2CO_3···CaO decomposition process shown in reactions 1 and 2, which in turn contributed to the higher CO_2 concentration at 700 °C.

CONCLUSIONS

The presence of CaO or $Ca(OH)_2$ in $Na_2CO_3\cdot H_2O$ lowered the decomposition temperature of Na_2CO_3, while the presence of SiO_2, Al_2O_3, and $CaCO_3$ did not show any effect. $Ca(OH)_2$ had a more pronounced effect than that of CaO, with the concentration, flow rate of sweep gas, and heating rate all affecting the decomposition temperature of Na_2CO_3. The formation of crystalline phases between CaO and Na_2CO_3 were not observed during heating in XRD, but the formation of $CaCO_3$-type species were observed. XPS studies also confirmed that the presence of CaO lowered the decomposition temperature of Na_2CO_3, with the formation of $Ca-CO_3$-type species observed during heating. The formation of carbonate-type species with CaO and Na_2CO_3 may have facilitated the decomposition of Na_2CO_3.

AUTHOR INFORMATION

Corresponding Author

*Telephone: 304-285-4513. Fax: 304-285-4403. E-mail: ranjani.siriwardane@netl.doe.gov.

ACKNOWLEDGMENT

The authors thank Dr. Robert Romanosky for his continued support throughout the years.

REFERENCES

(1) Goldeemberg, J.; Olende, S. A.; El-Ashry, M.; Davis, G.; Johansson, T.; Keith, D.; Jinghai, L.; Nakicenovic, N.; Pachauri, R.; Shafie-Pour, M.; Shpilrain, E.; Socolow, R.; Yamaji, K.; Luguang, Y. *Lighting the Way: Toward a Sustainable Energy Future*, Report; InterAcademy Council (IAC): Amsterdam, the Netherlands, Oct 2007.

(2) Energy Information Administration (EIA). *Greenhouse Gases, Climate Change, and Energy*; U.S. Department of Energy: Washington, D.C., 2008; Report DOE/EIA-X012.

(3) Skarstrom, C. W. Method and apparatus for fractionating gaseous mixtures by adsorption. U.S. Patent 2,944,627, 1960.

(4) Guerrin de Montgareuil, P.; Domine, D. Process for separating a binary gaseous mixture by adsorption. U.S. Patent 3,155,468, 1964.

(5) Van Kessel, L. B. M.; Saeijs, J. C. P. L.; Lalbahadoersing, V.; Arendsen, A. R. J.; Stavenga, M.; Heesink, A. B. M.; Temmink, H. M. G.

IGCC Power Plant: CO_2 Removal with High Temperature Adsorbents, Final Report; TNO: Delft, the Netherlands, April 1998; TNO Rapport R98/135.

(6) Golden, M. C.; Shivaji, S. Regenerative carbon dioxide (CO_2) removal system. U.S. Patent 6,322,612, 2001.

(7) Siriwardane, R. V. Regenerable sorbents for CO_2 capture from moderate and high temperature applications. U.S. Patent 7,314,847 B1, Jan 2008.

(8) Hassan, E. A.; Katib, S. M. A.; El-Qurashi, M. A. M.; El-Salaam, K. M. A. The doping effect of altervalent cations on the thermal decomposition and electrical conduction properties of manganese(II) carbonate. *J. Therm. Anal. Calorim.* **1994**, *41* (2−3), 337–346.

(9) Siriwardane, R. V.; Robinson, C.; Shen, M.; Simonyi, T. Novel regenerable sodium-based sorbents for CO_2 capture at warm gas temperatures. *Energy Fuels* **2007**, *21* (4), 2088–2097.

(10) Siriwardane, R. V.; Stevens, R. W., Jr. Novel regenerable magnesium hydroxide based sorbents for CO_2 capture at warm gas temperatures. *Ind. Eng. Chem. Res.* **2009**, *48* (4), 2135–2141.

(11) Wigmans, T.; Doorn, J. V.; Moulijn, J. A. Temperature-programmed desorption study of Na_2CO_3-containing activated carbon. *Fuel* **1983**, *62*, 190–195.

(12) Addoun, A.; Dentzer, J.; Ehrburger, P. Porosity of carbons obtained by chemical activation: Effect of the nature of the alkaline carbonates. *Carbon* **2002**, *40* (7), 1140–1143.

(13) Kim, J. W.; Lee, Y. D.; Lee, H. G. Decomposition of Na_2CO_3 by interaction with SiO_2 in mold flux of steel continuous casting. *ISIJ Int.* **2001**, *41*, 116–123.

(14) Said, A. A.; Hassan, E. A.; El-Salaam, K. M. A.; Mohamed, M. M. Influence of ion additions on the thermal decomposition of basic zinc carbonate. *J. Therm. Anal. Calorim.* **1990**, *36* (4), 1331–1345.

(15) Moulder, J. F.; Stickle, W. F.; Sobol, P. E.; Bomben, K. D. *Handbook of X-ray Photoelectron Spectroscopy*; Physical Electronics, Inc.: Eden Prairie, MN, 1992.

(16) Gelius, U.; Hedén, P. F.; Hedman, J.; Lindberg, B. J.; Manne, R.; Norberg, R.; Nordling, C.; Siegbahn, K. Molecular spectroscopy by means of ESCA III. Carbon compounds. *Phys. Scr.* **1970**, *2*, 70.

(17) Hammond, J. S.; Holubka, J. W.; Duckie; Devries, J. E. The application of X-ray photo-electron spectroscopy to a study of interfacial composition in corrosion-induced paint de-adhesion. *Corros. Sci.* **1981**, *21* (3), 239–253.

(18) Wagner, C. D.; Zatko, D. A.; Raymond, R. H. Use of the oxygen KLL lines in identification of surface chemical states by electron spectroscopy for chemical analysis use of the oxygen KLL lines in identification of surface chemical states by electron spectroscopy for chemical analysis. *Anal. Chem.* **1980**, *52*, 1445.

(19) Barrie, A.; Street, F. J. An auger and X-ray photoelectron spectroscopic study of sodium metal and sodium oxide. *J. Electron Spectrosc. Relat. Phenom.* **1977**, *7*, 1.

(20) Siriwardane, R. V.; Cook, J. M. Interactions of NO and SO_2 with iron deposited on silica. *J. Colloid Interface Sci.* **1985**, *104*, 250.

(21) Van Doveren, H.; Verhoeven, J. A. Th. XPS spectra of Ca, Sr, Ba and their oxides. *J. Electron Spectrosc. Relat. Phenom.* **1980**, *21* (3), 265.

(22) Franzen, H. F.; Merrick, J.; Umana, M.; Khan, A. S.; Peterson, D. T.; McCreary, J. R.; Thorn, R. J. XPS spectra and crystalline potentials in alkaline-earth chalco-genides and hydrides. *J. Electron Spectrosc. Relat. Phenom.* **1977**, *11*, 439.

(23) Landis, W. J.; Martin, J. R. X-ray photoelectron spectroscopy applied to gold-decorated mineral standards of biological interest. *J. Vac. Sci. Technol., A* **1984**, *2*, 1108.

(24) Christie, A. B.; Lee, J.; Sutherland, I.; Walls, J. M. An XPS study of ion-induced compositional changes with group II and group IV compounds. *Appl. Surf. Sci.* **1983**, *15*, 224.

(25) Siriwardane, R. V.; Poston, J. A., Jr.; Fisher, E. P.; Shen, M.-S.; Miltz, A. L. Decomposition of the sulfates of copper, iron(II), iron(III), nickel, and zinc: XPS, SEM, DRIFTs, XRD, and TGA study. *Appl. Surf. Sci.* **1999**, *152* (3−4), 219–236.

(26) Poston, J. A., Jr.; Siriwardane, R. V.; Fisher, E. P.; Miltz, A. L. Thermal decomposition of the rare earth sulfates of cerium(III) cerium-(IV), lanthanum(III) and samarium(III). *Appl. Surf. Sci.* **2003**, *214* (104), 83–102.